Ecological Modelling 267 (2013) 93–101

Contents lists available at ScienceDirect

Ecological Modelling

journal homepage: www.elsevier.com/locate/ecolmodel

Short communication

Impact of parameter choice on the dynamics of NPZD type ecosystem models

A. Heinle*, T. Slawig

Cluster "The Future Ocean", Institute of Computer Science, Christian-Albrechts University, 24098 Kiel, Germany

ARTICLE INFO

Article history:
Received 30 March 2013
Received in revised form 18 July 2013
Accepted 20 July 2013

Keywords:
Marine ecosystem models
Parameters
Qualityof solutions
Limit cycles

ABSTRACT

Marine ecosystem models of NPZD type are analyzed to identify model specific dynamics in dependence on the parameter setting used. It is shown that detecting the equilibria of a model and computing the eigenvalues of its linearizations it is possible to completely determine its dynamics. Three related model formulations are analyzed this way. Based on analytical computations for the simplest formulation, a theoretical classification of the occurrence of specific dynamics is presented. Its significance for all three model formulations is examined using numerical methods. Further, dynamical characteristics arising from the enhancemet of complexity in the model formulation are examined. Similarities and differences of the three models are pointed out. The most significant dynamical discrepancy is that the simplest model formulation shows limit cycles while this feature does not appear in the other two models. The results presented in this study show that knowing the basic dynamics of a model its valid application can be ensured.

1. Introduction

Nowadays, several approaches exist to model the marine ecosystem in the research of climate change (see e.g. Oschlies and Garçon, 1999; Moore et al., 2002; Gregg et al., 2003; Fasham et al., 2006). To determine whether a model is suitable for a given task or not, data assimilation techniques are frequently applied. Thereby, the model parameters are tuned or optimized to the effect that the model outcome fits observational data that represents the system to be simulated (see e.g. Fennel et al., 2001; Schartau and Oschlies, 2003; Rückelt et al., 2010; Kidston et al., 2011). One drawback of this method however is obvious. The model to data misfit may be reduced by such methods, but nothing is gained about the models general behaviour. The question, whether the model actually depicts the dynamics of the system considered is not addressed this way.

In this study, a theoretical approach is presented to reveal the basic dynamics of a model to ensure its legitimate application. Model dynamics are determined by its mathematical framework. In marine ecosystem modelling, such a framework is usually given by a system of coupled ordinary or partial differential equations which describe the temporal development of the modelled components (Fennel et al., 2004). As the mathematical theory of differential equations, especially the theory of ordinary differential equations (ODEs), is well-established, this theory can be used for a theoretical investigation of the dynamics of marine ecosystem models.

Here, the proposed method is presented for NPZD type models. Simulating the concentration of the four major components of marine ecosystems nutrients (N), phytoplankton (P), zooplankton (Z) and detritus (D), NPZD type models belong to the marine ecosystem models of medium complexity. They are frequently used in climate research because the consideration of these four variables has the benefit that, on the one hand, a certain amount of realism is ensured, on the other hand, the number of parameters included, thus, the degrees of freedom in the model, has a manageable size. The actual complexity of the model, of course, depends on its explicit mathematical formulation.

To study the effect of small variations on the model dynamics, three hierarchically structured model formulations, introduced in our previous study Heinle and Slawig (2013), are analyzed, where the difference between the single formulations is in their individual representation of phytoplankton and zooplankton loss. While in our earlier study the equilibria of the model formulations are introduced and the effect of diverse amounts of nitrogen in the system is discussed, in this study, the effect of parameter variations is examined. Critical parameters and parameter constellations are exposed whose knowledge allows the controlled application of the model and helps to interpret the respective results.

In the following section, the three model formulations analyzed in this study are shortly introduced and in Section 3, the results

* Tel.: +49 431 880 7338; fax: +49 431 880 7618.
E-mail address: ahe@informatik.uni-kiel.de (A. Heinle).
URL: http://www.informatik.uni-kiel.de/co2 (A. Heinle).

0304-3800/$ – see front matter © 2013 Elsevier B.V. All rights reserved.
http://dx.doi.org/10.1016/j.ecolmodel.2013.07.019

achieved by our proposed theoretical analysis are given. Firstly, the equilibria of the ODE systems introduced in Heinle and Slawig (2013) are shortly regiven as well as some stability statements are noted. Then, a classfication of the solutions stability dependent on crucial parameter constellations, deduced from our theoretical analysis, is presented for the simplest model formulation, model LLM. In Section 4, the analytic results are expanded by numerical calculations. For all three models, the effect of parameter variations is figured out. Comperative calculations are performed to highlight differences and similarities of the individual model formulations. A summary and conclusions complete the study in Sections 5 and 6.

2. Models

In this study, the dynamical effect of parameter variations is investigated for three NPZD type model formulations introduced in Heinle and Slawig (2013). All three models, model LLM, LQM and QQM, simulate the concentrations of nutrients (N), phytoplankton (P), zooplankton (Z) and detritus (D) in (mmol N m^{-3}), but they differ in the representation of phytoplankton loss and zooplankton loss.

The governing equations for model LLM and model LQM are given by the ODE system

$$\begin{aligned}\frac{\partial N}{\partial t} &= -J(N,I)P + \phi_Z Z + \gamma_m D\\ \frac{\partial P}{\partial t} &= (J(N,I) - \phi_P)P - G(\epsilon,g,P)Z\\ \frac{\partial Z}{\partial t} &= (\beta G(\epsilon,g,P) - \phi_Z - \phi_Z^* Z)Z\\ \frac{\partial D}{\partial t} &= \phi_P P + ((1-\beta)G(\epsilon,g,P) + \phi_Z^* Z)Z - \gamma_m D,\end{aligned} \tag{2.1}$$

where we refer to model LLM in case $\phi_Z^* = 0$. The system of governing equations for model QQM is given by

$$\begin{aligned}\frac{\partial N}{\partial t} &= (-J(N,I) + \phi_P)P + \phi_Z Z + \gamma_m D\\ \frac{\partial P}{\partial t} &= (J(N,I) - \phi_P - \phi_P^* P)P - G(\epsilon,g,P)Z\\ \frac{\partial Z}{\partial t} &= (\beta G(\epsilon,g,P) - \phi_Z - \phi_Z^* Z)Z\\ \frac{\partial D}{\partial t} &= \phi_P^* P^2 + ((1-\beta)G(\epsilon,g,P) + \phi_Z^* Z)Z - \gamma_m D.\end{aligned} \tag{2.2}$$

It can be seen that Eqs. (2.1) and (2.2) coincide except the representation of phytoplankton loss and zooplankton loss. Model LLM considers only linear loss of both variables. Model LQM includes an additional quadratic loss term of zooplankton and model QQM has linear and quadratic loss terms of both variables. In both systems of equations the functions J and G describe the growth of phytoplankton and the grazing of zooplankton, respectively, which are defined as

$$J(N,I) = \mu_m \cdot \frac{N}{k_N + N} \cdot \frac{I}{k_I + I}$$

and

$$G(\epsilon,g,p) = \frac{g\epsilon p^2}{g + \epsilon p^2}.$$

The parameters included in the ODE systems and functions above are defined and explained in Table 1. For further details, especially on the functions J and G, we refer to Heinle and Slawig (2013).

3. Analytical calculations

In this chapter, the analytic results of our work are shown. For completeness, the parameter and initial value dependent equilibrium solutions of the three models, introduced in Heinle and Slawig (2013), are shortly regiven. Then, stability statements of these solutions are presented, which are based on a linearization approach, and crucial parameter and initial value constellations are figured out.

3.1. Equilibrium solutions

The *reasonable*, meaning non-negative and real-valued, equilibrium solutions found for model LLM, LQM and QQM are shortly regiven in the following. Thereby, the concentrations of the four state variables are summarized in the vector $y = (N, P, Z, D)$ and the sum of the four positive initial values y_0 is summarized in the variable $S = \sum y_0^i$. When speaking about the parameters included in the governing equations (Eqs. (2.1) and (2.2), respectively), we refer to $u \in \mathbb{R}^m$, where m is the number of parameters included in the respective system of equations. When a specific parameter is addressed, its symbol in accordance with Table 1 is noted.

3.1.1. Model LLM and LQM

Each model has three reasonable equilibrium solutions. For model LLM and LQM the first and second equilibria are

$$E^*_{LLM_1} = E^*_{LQM_1} = (N^*(S), 0, 0, 0) \tag{3.1}$$

and

$$E^*_{LLM_2} = E^*_{LQM_2} = \left(\frac{k\phi_P}{\mu_m - \phi_P}, P_2^*(S,u), 0, \frac{\phi_P}{\gamma} P_2^*(S,u)\right) \tag{3.2}$$

with

$$P_2^*(S,u) = \frac{S - k\phi_P/(\mu_m - \phi_P)}{(\phi_P\gamma) + 1}. \tag{3.3}$$

For model LLM, the third equilibrium is given by

$$E^*_{LLM_3} = (N_3^*(S,u), P_3^*(u), Z_3^*(S,u), D_3^*(S,u)) \tag{3.4}$$

with

$$P_3^*(u) = \sqrt{\frac{\phi_Z g}{\epsilon(\beta g - \phi_Z)}} \tag{3.5}$$

and for model LQM

$$E^*_{LQM_3} = \left(N_3^*(S,u), P_3^*(S,u), Z_3^*(S,u), D_3^*(S,u)\right). \tag{3.6}$$

The explicit state expressions of $N_3^*(S,u)$, $Z_3^*(S,u)$ and $D_3^*(S,u)$ of solution $E^*_{LLM_3}$ are given in the Appendix due to their complexity. The ones of $E^*_{LQM_3}$ are not any more given.

3.1.2. Model QQM

For model QQM, there are also three reasonable equilibrium solutions. The first one equals the one of the other two models (see Eq. (3.1)), the second equilibrium is given by

$$E^*_{QQM_2} = \left(N^*(S,u), P^*(S,u), 0, \frac{\phi_P^*}{\gamma} P^*(S,u)^2\right), \tag{3.7}$$

with

$$N_2^*(S,u) := \frac{k(\phi_P + \phi_P^* P^*(S,u))}{\mu_m - (\phi_P + \phi_P^* P^*(S,u))} \tag{3.8}$$

and the third equilibrium of model QQM is described by the same general formulation as $E^*_{LQM_3}$ (see Eq. (3.6)). Its explicit expression however is not given.

Table 1
Units and definitions of the variable model parameters in mmol N m^{-3} as well as exemplary parameter set u_{opt} introduced in Schartau and Oschlies (2003).

Symbol	Range	u_{opt}	Unit	Definition
β	[0,1]	0.925	1	Assimilation efficiency of zooplankton
μ_m	$\mathbb{R}_+$	0.270	d^{-1}	Phytoplankton growth rate
ϕ_P	$\mathbb{R}_+$	0.040	d^{-1}	Phytoplankton linear loss rate
ϕ_P^*	$\mathbb{R}_+$	0.025	d^{-1}	Phytoplankton quadratic loss rate
ϵ	$\mathbb{R}_+$	1.600	m^6 (mmol N)$^{-2}$ d^{-1}	Grazing encounter rate
g	$\mathbb{R}_+$	1.575	d^{-1}	Maximum grazing rate
ϕ_Z	$\mathbb{R}_+$	0.010	d^{-1}	Zooplankton linear loss rate
ϕ_Z^*	$\mathbb{R}_+$	0.340	m^3 (mmol N)$^{-1}$ d^{-1}	Zooplankton quadratic loss rate
γ_m	$\mathbb{R}_+$	0.048	d^{-1}	Detritus remineralization rate
k_N	$\mathbb{R}_+$	0.700	mmol N m^{-3}	Half saturation constant for NO_3 uptake
k_I	$\mathbb{R}_+$		W m^{-3}	Half saturation constant for light

Note that all three equilibria of model LLM are analytically calculable, while the solutions $E^*_{LQM_3}$, $E^*_{QQM_2}$ and $E^*_{QQM_3}$ need numerical methods for computation.

3.2. Quality of equilibria

The quality of an equilibrium solution in terms of its stability properties determines the way the solution influences the systems behaviour. While stable solutions are attractive, meaning the system tends towards this solution, the system drifts away from unstable solutions. In this section, the quality of the previously introduced equilibrium solutions subject to critical parameters is presented. As far as possible analytical calculations are done (cp. Section 3.1), otherwise numerical methods are used.

3.2.1. Quality analysis of nonlinear systems

There are two main approaches to analyze the quality of nonlinear systems. One is based on the *Lyapunov theory*, the other one is based on linearizations. A clear advantage of the Lyapunov theory is its global validity. Statements based on linearizations are in contrast only locally validated. In practice, however, it is often difficult to use the former because it requires the creation of so-called Lyapunov functions, a task, highly challenging for the most realistic applications and sometimes even impossible. For that reason, the linearization approach is applied in this study.

Given a differentiable function $f : \mathbb{R}^n \to \mathbb{R}^n$ and an equilibrium y^*, the *linearization* of a nonlinar autonomous ODE system $y' = f(y)$ in y^* is given by

$$\bar{y}' = J_f(y^*)\ \bar{y}(t), \tag{3.9}$$

where $J_f(y^*)$ is the Jacobian of f evaluated at the point y^*. This linearization has locally the same quality properties as the original nonlinear ODE system (Amann, 1990). For linear systems the quality of an equilibrium is determined by the eigenvalues $\lambda = \alpha + i\beta$ of the governing matrix, in the case of linearizations, by the eigenvalues of the matrix $J_f(y^*)$. In case all eigenvalues λ have negative real parts, the equilibrium solution y^* is called stable. In case the real part of at least one eigenvalue is positive, the equilibrium solution y^* is called to be unstable. Note that these are global statements with respect to the linearized system (3.9), but local statements with respect to the nonlinear system. In case the real part of the maximum eigenvalue is 0, there are theoretical statements about the solutions quality for the linearized system, but nothing can be concluded on its quality in the nonlinear system.

In the following we call a solution y^* *linearized stable* (*unstable*) if the solution is stable (unstable) with respect to its linearization.

3.2.2. Quality statements

The quality of equilibrium solution $E^*_{LLM_1}$ (Eq. (3.1)), which is the same for all three models, as well as the quality of solution $E^*_{LLM_2}$ (Eq. (3.2)) can be analyzed analytically. The other solutions are too complicated to allow for analytic computations (cp. Section 3.1). In this section, we mostly refer to model LLM, but all results with respect to solution $E^*_{LLM_1}$ are equally valid for model LQM and model QQM because the linearizations in $E^*_{LLM_1}$ are independent of the underlying ODE System (cp. J_{QQM} in Appendix A).

The linearizations of model LLM are determined by the Jacobian of Eq. (2.1) with $\phi_Z^* = 0$,

$$J_{LLM} = \begin{pmatrix} -\frac{\mu_m k_N P}{(k_N+N)^2} & -\frac{\mu_m N}{k_N+N} & \phi_Z & \gamma \\ \frac{\mu_m k_N P}{(k_N+N)^2} & \frac{\mu_m N}{k_N+N} - \phi_P - \frac{2g^2\epsilon PZ}{(g+\epsilon P^2)^2} & -\frac{g\epsilon P^2}{g+\epsilon P^2} & 0 \\ 0 & \frac{\beta 2g^2\epsilon PZ}{(g+\epsilon P^2)^2} & \frac{\beta g\epsilon P^2}{g+\epsilon P^2} - \phi_Z & 0 \\ 0 & \frac{(1-\beta)2g^2\epsilon PZ}{(g+\epsilon P^2)^2} + \phi_P & \frac{(1-\beta)g\epsilon P^2}{g+\epsilon P^2} & -\gamma \end{pmatrix}.$$

Integrating $E^*_{LLM_1}$ in J_{LLM} provides the constant matrix

$$J_{LLM}(E^*_{LLM_1}) = \begin{pmatrix} 0 & -\frac{\mu_m S}{k_N+S} & \phi_Z & \gamma \\ 0 & \frac{\mu_m S}{k_N+S} - \phi_P & 0 & 0 \\ 0 & 0 & -\phi_Z & 0 \\ 0 & \phi_P & 0 & -\gamma \end{pmatrix},$$

which has the eigenvalues

$$\lambda_{LLM_1} = \left(0, -\phi_Z, -\gamma, -\frac{k_N\phi_P - \mu_m S + \phi_P S}{k_N + S}\right). \tag{3.10}$$

In our models, $u > 0$ is postulated. Thus, the real parts of the second and third eigenvalues of Eq. (3.10), λ^2 and λ^3, are negative given any initial mass S and parameter setting u. The fourth eigenvalue, however, can be positive or negative.

Based on the real part of the maximum eigenvalue, the following statement can be derived for equilibrium $E^*_{LLM_1}$.

Proposition 3.1. *If $\mu_m > \phi_P$, then $E^*_{LLM_1}$ is locally unstable for all initial masses $S > k_N\phi_P/(\mu_m - \phi_P)$.*

As the maximum eigenvalue has zero real part in case $\lambda^4 < 0$, an equivalent direct statement on the local stability of solution $E^*_{LLM_1}$ cannot be deduced. For linear systems, however, an equilibrium solution is proven to be stable also when the real part of the maximum eigenvalue equals zero and the multiplicity of this eigenvalue is one (cp. Amann, 1990). This is true in the present case and we state the following.

Proposition 3.2. *If $\mu_m \le \phi_P$, then $E^*_{LLM_1}$ is stable for all initial masses S with respect to its linearized system.*

Criteria for the quality of the other two equilibria cannot be obtained since the expressions of the respective eigenvalues are too

Table 2
Classification of the equilibrum solutions for model LLM. Shown are the potentially stable solutions according to our analytical findings. On the left, the constellations given $\mu_m > \phi_P$ are shown (A), on the right for $\mu_m \leq \phi_P$ (B). The combination $\mu_m \leq \phi_P$ and $S \leq k\phi_P/(\mu_m - \phi_P)$ results in a contradiction to $S > 0$ and is marked by '–'.

A			B		
$\mu_m > \phi_P$	$S > k\phi_P/(\mu_m - \phi_P)$	$S \leq k\phi_P/(\mu_m - \phi_P)$	$\mu_m \leq \phi_P$	$S > k\phi_P/(\mu_m - \phi_P)$	$S \leq k/(\mu_m - \phi_P)$
$\beta g > \phi_Z$	$E^*_{LLM_2}$ or $E^*_{LLM_3}$	$E^*_{LLM_1}$	$\beta g > \phi_Z$	$E^*_{LLM_1}$	–
$\beta g \leq \phi_Z$	$E^*_{LLM_2}$	$E^*_{LLM_1}$	$\beta g \leq \phi_Z$	$E^*_{LLM_1}$	–

nested to support constructive conclusions. However, the eigenvalues of the linearization in $E^*_{LLM_2}$

$$J_{LLM}(E^*_{LLM_2}) = \begin{pmatrix} -\psi_1 & -\phi_P & \phi_Z & \gamma \\ \psi_1 & 0 & -g + \psi_2 & 0 \\ 0 & 0 & \beta g - \phi_Z - \beta\psi_2 & 0 \\ 0 & \phi_P & (1-\beta)g - (1-\beta)\psi_2 & -\gamma \end{pmatrix},$$

where

$$\psi_1 = \frac{\gamma(\phi_P - \mu_m)(k_N\phi_P + \phi_P S - \mu_m S)}{k_N\mu_m(\gamma + \phi_P)}$$

and

$$\psi_2 = \frac{g^2}{g + \frac{\epsilon\gamma^2(S+(k_N\phi_P/(\phi_P-\mu_m)))^2}{\phi_P^2((\gamma/\phi_P)+1)^2}}$$

are still symbolically computable and as for λ_{LLM_1}, one of these eigenvalues equals zero (cp. Eq. (3.10)).

3.2.3. Classification

From the analytical expressions detected and presented, explicit parameter and initial value constellations are derived that decide on the reaosnability and quality of the equilibrium solutions. For model LLM, critical parameter constellations are exposed for all three equilibria $E^*_{LLM_1}$, $E^*_{LLM_2}$ and $E^*_{LLM_3}$. This enables the introduction of a classification of the solutions occurrence dependent on these constellations (see Table 2). On the left, the possible combinations with $\mu_m > \phi_P$ are posed, on the right the ones including $\mu_m \leq \phi_P$. As a co-occurrence of $\mu_m \leq \phi_P$ and $S \leq k_N\phi_P/(\mu_m - \phi_P)$ is in contradiction to $S > 0$, this case is marked by '–'.

In this classification, all analytical findings are integrated. Especially Proposition 2, which is a statement with respect to the linear approximation of model LLM, contributes to the decision whether $E^*_{LLM_1}$ or one of the other equilibria occurs in some cases (cp. Table 2, B). Consequently, the classification presented is theoretically founded for the linearized system and not for model LLM itself (cp. the previous section). Thus, to identify its significance with respect to model LLM, numerical experiments are conducted.

4. Numerical computations

To identify the stability properties of model LLM, LQM and QQM and especially, to see how far these properties coincide with the ones presented above for the linear approximation of model LLM, numerical computations are done. Since the analytical results indicate the primary importance of the parameters k_N, μ and ϕ_P, but also of the parameters ϕ_Z, β, g and ϕ^*_P for the equilibrium solutions of the models and their stability, we present computations where some of these parameters are varied. Due to the conformity of our model formulations with the one presented in Schartau and Oschlies (2003), the ranges the parameters are varied are around a parameter setting presented therein (see u_{opt} in Table 1). The effect of variations in parameters mentioned above but not explicitly shown in the following can be easily deduced comparing the constellations presented in Table 2.

4.1. Coincidence of analytical and numerical computations

To show the significance of the results presented in this section, the coincidence of equilibrium solutions obtained from numerical model integrations and analytical calculations is shown at first. Therefore, the models are numerically solved using a Runge–Kutta method for 5 model years to reach equilibrium state. Then, the linearizations in these equilibrium states are determined and the eigenvalues are numerically computed using the MATLAB built-in function `eig`. These eigenvalues are compared with analytically computed eigenvalues. Those are also obtained by the routine `eig`, but for symbolic expressions.

Table 3 shows the real parts α of the analytically computed non-zero eigenvalues of the linearizations $J_{LM}(E_{LLM_1})$, $J_{LM}(E_{LLM_2})$ and $J_{LM}(E_{LLM_3})$ as well as the eigenvalues real parts of the linearization $J_{LM}(E_{LLM_{num}})$ where $E_{LLM_{num}}$ are the numerically obtained equilibrium states. Looking at those, it can be seen that the numerically computed eigenvalues $\lambda_{LLM_{num}}$ always coincide with one of the analytical eigenvalues λ_{LLM_i}, $i \in 1, 2, 3$. For small values of ϕ_P, the numerically based eigenvalues equal the ones calculated for the analytical solution $E^*_{LLM_3}$. For values ϕ_P larger than $\phi_P \sim 0.811$, the numerical eigenvalues confirm the ones of the analytic linearization in $E^*_{LLM_2}$ for a short period, and from values around $\phi_P \sim 0.815$ up to the maximum value of ϕ_P considered in this study, the numerical based eigenvalues coincide with the ones of the linearization $J_{LM}(E^*_{LLM_1})$.

For model LQM and model QQM, the coincidence of analytical – as far as they exist – and numerical computations is checked the same way.

4.2. Dynamics of model LLM

The classification presented in Table 2 is theoretically based for the linearizations of model LLM, but not for the nonlinear system underlying model LLM. Therefore, numerical experiments are conducted to estimate the extent to which the properties stated in this classification hold for the original nonlinear system.

The equilibria and eigenvalues for model LLM, presented in Section 3, are computed for given parameter and initial value settings using the software MATLAB and MUPAD. As long as analytical expressions exist, this is done symbolically to prevent rounding errors and to enable the detection of critical values. Otherwise, equilibria that are numerically computed serve as a base for the computations. Results are presented for variations of parameter set u_{opt} as introduced in Section 4. The variation in ϕ_P and the variation in ϕ_Z are discussed in more detail, while the results with respect to the variations in μ_m and k_N are only briefly mentioned, because they do not show new characteristic dynamics.

4.2.1. Variation in ϕ_P

Fig. 1 shows the results of the variation in ϕ_P. At the top, the concentrations of the states in equilibrium, obtained from numerical integrations, are illustrated. Below, the real parts of the corresponding maximum eigenvalues λ^{max} are shown. In all three plots, critical points $C(\phi_P)$ that are derived from Table 2 are marked by vertical lines. In particular, the dash–dotted line corresponds to the critical point $C_1(\phi_P)$ determined by the equation $k_N\phi_P/(\mu_m - \phi_P) - S = 0$

Table 3
Real parts of the non-zero eigenvalues for model LLM for initial mass $S = 15$ mmol N m^{-3} and parameter set u_{opt}, where parameter ϕ_P is varied. λ_{LLM_1}, λ_{LLM_2} and λ_{LLM_3} are the analytically calculated eigenvalues, $\lambda_{LLM_{num}}$ is calculated for the equilibrium solution obtained solving the model numerically.

	ϕ_P	α		
λ_{LLM_1}	0	−0.010000	−0.048000	0.815052
	0.2	−0.010000	−0.048000	0.615052
	...			
	0.8	−0.010000	−0.048000	0.015052
	0.81	−0.010000	−0.048000	0.005052
	0.812	−0.010000	−0.048000	0.003052
	0.814	−0.010000	−0.048000	0.001052
	0.816	−0.010000	−0.048000	−0.000948
	...			
	0.85	−0.010000	−0.048000	−0.034948
	0.9	−0.010000	−0.048000	−0.084948
λ_{LLM_2}	0	1.440529	−18.280441	−0.048000
	0.2	1.290550	−1.812290	−0.279708
	...			
	0.8	0.078265	−0.024595	−0.024595
	0.81	0.005526	−0.041739	−0.006581
	0.812	−0.003758	−0.044640	−0.003544
	0.814	−0.009182	−0.046956	−0.001105
	0.816	−0.009263	−0.048857	0.000909
	...			
	0.85	1.431156	−0.050542	0.002694
	0.9	0.977659	−0.026653	−0.026653
λ_{LLM_3}	0	−0.758001	−0.021711	−0.048131
	0.2	−0.567228	−0.021575	−0.048411
	...			
	0.8	−0.008174	−0.008174	−0.042657
	0.81	−0.043421	−0.004403	−0.000520
	0.812	−0.043536	−0.008052	0.005183
	0.814	−0.043646	−0.009668	0.008847
	0.816	−0.043750	0.011991	−0.010770
	...			
	0.85	0.050745	−0.016337	−0.044939
	0.9	0.102012	−0.018200	−0.045837
$\lambda_{LLM_{num}}$	0	−0.758001	−0.021711	−0.048131
	0.2	−0.567228	−0.021575	−0.048411
	...			
	0.8	−0.008174	−0.008174	−0.042657
	0.81	−0.043421	−0.004403	−0.000520
	0.812	−0.044640	−0.003544	−0.003758
	0.814	−0.001105	−0.046956	−0.009182
	0.816	−0.000948	−0.048000	−0.010000
	...			
	0.85	−0.034948	−0.048000	−0.010000
	0.9	−0.084948	−0.048000	−0.010000

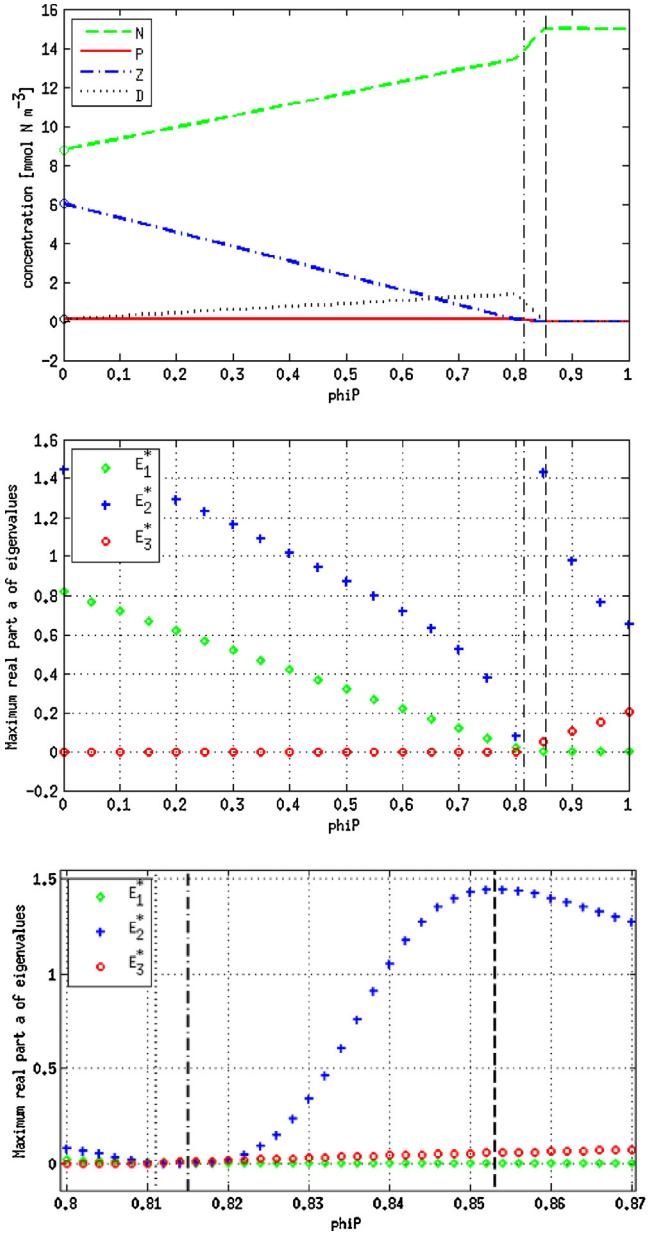

Fig. 1. Concentrations in equilibrium for model LLM (top) and the eigenvalues highest real part of the linearizations $J_1(E^*_{LLM_1})$, $J_1(E^*_{LLM_2})$ and $J_1(E^*_{LLM_3})$ (centre and bottom) for initial mass $S = 15$ mmol N m^{-3} and parameter set u_{opt}, plotted as functions of the linear mortality rate of phytoplankton ϕ_P. Vertical lines mark the critical points determined in accordance to analytical findings. Concentrations are obtained running the model for 5 model years. Eigenvalues are symbolically calculated.

(cp. also Eq. (3.3)). The dashed line corresponds to the critical point $C_2(\phi_P)$ at which $\mu_m - \phi_P = 0$ (cp. also Eq. (3.2)). A third critical point $C_3(\phi_P) \sim 0.811$, marked by a dotted line, is only shown in the bottom plot due to its proximity to $C_2(\phi_P)$. This point is not taken from Table 2, but is related to the eigenvalues of linearization $J_1(E^*_{LLM_2})$. Due to the high interlacing of those eigenvalues, an explicit expression of $C_3(\phi_P)$ cannot be given, its analytical calculation however is possible.

Looking at the top plot of Fig. 1, it can be seen that the equilibrium state of each variable changes continuously with varying phytplankton mortality rate ϕ_P. Not visible in that plot, but noticable in the plot at the bottom, a first change of the solutions quality occurs at the critcal point $C_3(\phi_P)$. For $\phi_P \leq C_3(\phi_P)$ numerical solutions converge to E_{LLM_3}. From then on, numerical solutions end in solution E_{LLM_2} for a short period and at $C_1(\phi_P)$, the solutions quality changes again and $E^*_{LLM_1}$ is stable for all $\phi_P > C_1(\phi_P)$ as indicated by our classification. The critical value $C_2(\phi_P)$ is not crucial for the presented parameter and initial value setting.

Looking at the two bottom plots of Fig. 1, that show the maximum eigenvalues of the three equilibrium solutions, it is obvious that for all linearizations, the maximum eigenvalue λ^{max} is positive or zero. particularly, always one linearization shows $\lambda^{max} = 0$, while the others have at least one eigenvalue $\lambda > 0$. The latter implies the instability of the associated solution with respect to the linearization as well as with respect to the original nonlinear system. For the former however, nothing can be concluded from the theory. But comparing the two top plots of Fig. 1, it is obvious, that numerical solutions converge to the equilibrium whose linearization has $\lambda^{max} = 0$ and thus, this solution is stable with respect to the nonlinear system as well.

4.2.2. Variation in ϕ_Z

The variation in ϕ_Z shows a new characteristic of model LLM. Some parameter constellations result in periodic solutions,

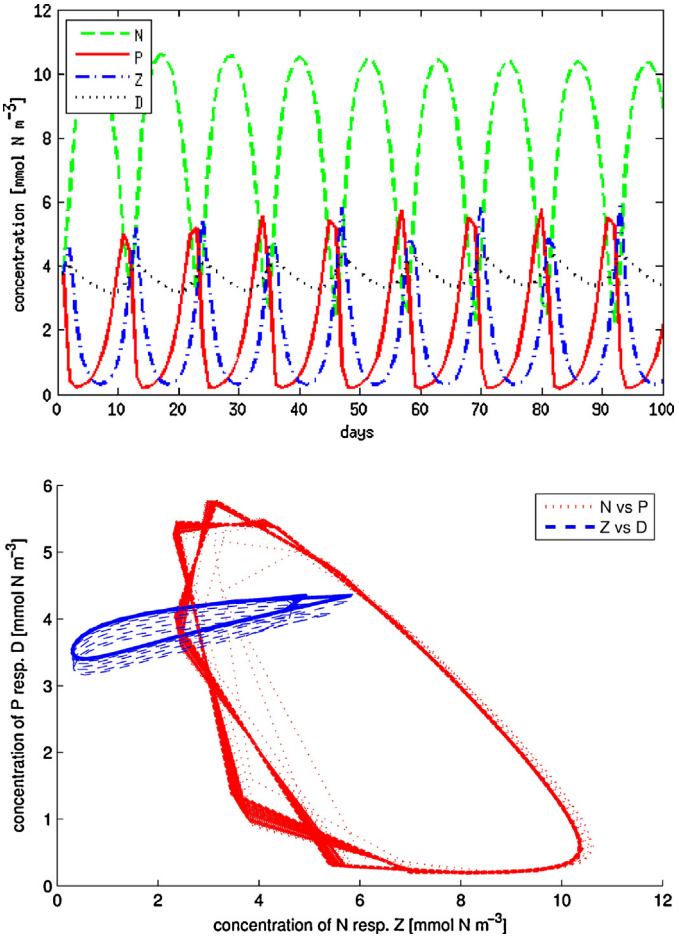

Fig. 2. Solution of model LLM for initial mass $S = 15$ mmol N m^{-3} and parameter set u_{opt} with $\phi_Z = 0.75$. All three equilibria presented in Section 3.1 are unstable and instead, a stable limit cycle occurs around $E^*_{LLM_3}$. The top plot shows the states of N, p, Z and D over time, the bottom plot shows the phase curves N vs. p and Z vs. D.

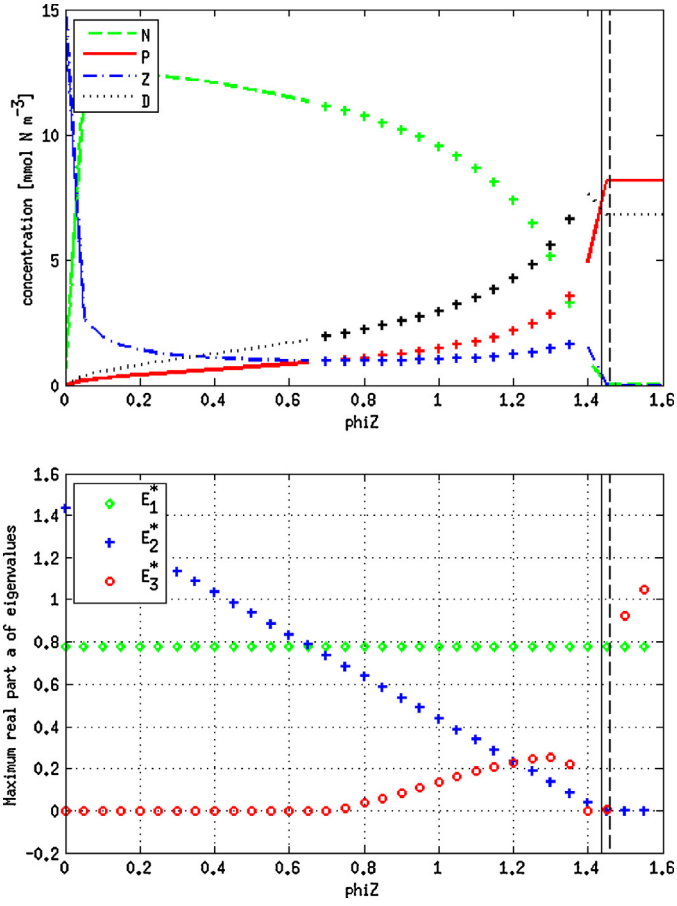

Fig. 3. Concentrations in equilibrium for model LLM (top) and the eigenvalues highest real part of the linearizations $J_1(E^*_{LLM_1})$, $J_1(E^*_{LLM_2})$ and $J_1(E^*_{LLM_3})$ (bottom) for initial mass $S = 15$ mmol N m^{-3} and parameter set u_{opt}, plotted as functions of the linear mortality rate of zooplankton ϕ_Z. Vertical lines mark the critical points determined in accordance to analytical findings. Crosses in the top plot mark analytically determined equilibrium solutions in the range no equilibrium is stable. Lines depict the range numerical equilibrium solutions are obtained after 5 model years. Eigenvalues are symbolically calculated.

so-called limit cycles. An example, a limit-cycle with period 2, is shown in Fig. 2, obtained for $S = 15$ mmol N m^{-3} and u_{opt} with $\phi_Z = 0.75$. The upper plot shows the periodic behaviour over time, the lower plot shows the corresponding phase curves N vs. p and Z vs. D.

The whole variation in ϕ_Z is illustrated in Fig. 3, which is similar to Fig. 1. While the top plot illustrates the equilibrium solutions, the bottom plot shows the real parts of the maximum eigenvalues of the respective linearizations in E_{LLM_i}, $i = 1, 2, 3$, but here as functions of ϕ_Z. Looking at the bottom plot, it can be seen, that for ϕ_Z, in contrast to the variation previously discussed, a domain D_{cycle} exists where all three linearizations have an eigenvalue with a positive real part α. This means that all three equilibria are unstable as $\phi_Z \in D_{cycle}$, which especially holds for both, the linearizations and model LLM and that results in the above mentioned limit cycles. In the upper plot, lines depict the equilibrium states in the range of $\phi_Z \notin D_{cycle}$, where numerical solutions converge to these states. In the range the model does not converge to one of the equilibrium solutions presented in Section 3.1, crosses mark analytically computed solutions of E_{LLM_3} because the arising limit cycles oscillate around this equilibrium (cp. Fig. 2).

The critical points, on the one hand the value of ϕ_Z where equilibrium E_{LLM_3} becomes unstable and the model solution starts to oscillate around E_{LLM_3} and on the other hand, the point where the limit cycle breaks down and solution E_{LLM_3} becomes stable again, are not exactly determinable. These critical points depend solely on the eigenvalues of linearization $J_1(E^*_{LLM_3})$, whose symbolic expressions are not detectable. Two other critical points are explicit detectable, namely $C_1(\phi_Z)$, marked by a dashed line in Fig. 3 and resulting from the equality $\phi_Z - \beta g = 0$ (cp. Eq. (3.5)) and $C_2(\phi_Z)$ which arises from one of the eigenvalues λ_{LLM_2} (cp. variation in ϕ_P) and which is marked by a solid line in Fig. 3. While in the present example $C_1(\phi_Z)$ has no effect on the solution of model LLM, a quality shift from solution E_{LLM_3} to solution E_{LLM_2} occurs at $C_2(\phi_Z) \sim 1.4357$ (cp. Fig. 3). The maximum eigenvalue of λ_{LLM_1} is constant because these eigenvalues are not effected by ϕ_Z.

4.2.3. Variations in k_N and μ_m

Parameter variations of u_{opt} in k_N and μ_m show similar results as presented for ϕ_P. A variation in k_N does not lead to a quality change of the three solutions. Using u_{opt}, E_{LLM_3} is stable up to very high values of k ($k > 100$). Variations in μ_m show that equilibrium $E^*_{LLM_1}$ is stable for very small values of μ_m, while from $C_1(\mu) \sim 0.042$, derived from the equation $k_N \phi_P / (\mu_m - \phi_P) - S = 0$, equilibrium E_{LLM_3} is stable.

Given any situation, the results of numerical experiments for model LLM are in accordance with the classification introduced in Table 2. This is also true when using other parameter settings as a base and thus, it is indicated that the classification holds for the non-linear system (2.1). The numerical investigations showed

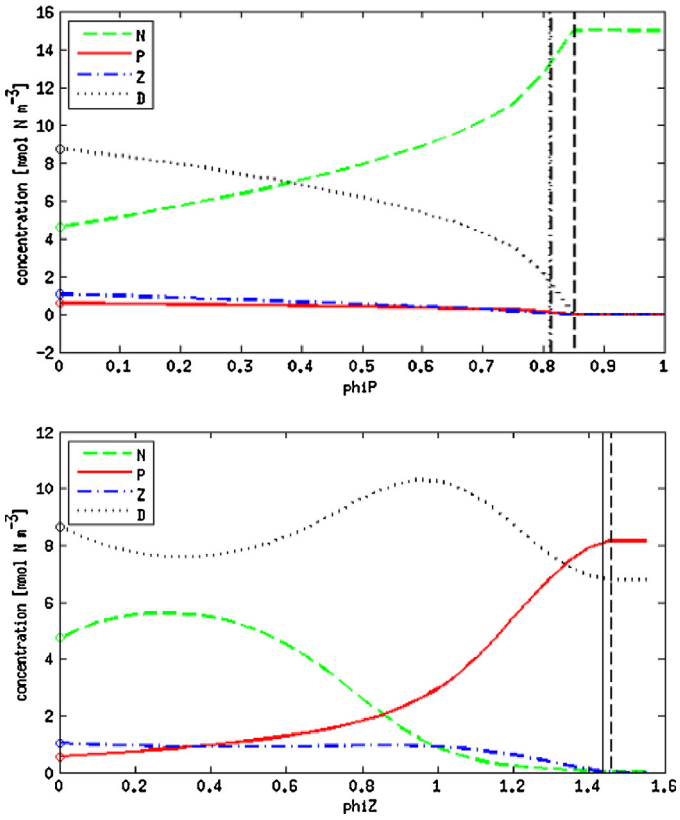

Fig. 4. Concentrations in equilibrium for model LQM for an initial mass $S = 15$ mmol N m^{-3} and parameter set u_{opt}, plotted as a function of the linear mortality rate of phytoplankton ϕ_P (top) and as function of the linear mortality rate of zooplankton ϕ_Z (bottom). Vertical lines mark the critical values $C(\phi_P)$ and $C(\phi_Z)$ in accordance to Fig. 1. Equilibria are obtained running the model for 5 model years.

additionally that limit cycles can occur around solution $E^*_{LLM_3}$, a feature that is analytically not detectable.

4.3. Dynamics of model LQM and model QQM

For model LQM and model QQM we have less analytical results than for model LLM. In particular, we do not have explicit solutions for the equilibrium solutions $E^*_{LQM_3}$, $E^*_{QQM_2}$ and $E^*_{QQM_3}$. But the analytical results presented for model LLM are appropriate to be used as a base for the investigation of the dynamics of model LQM. That is because the models differ only in a term that includes the state of Z and it holds $Z = 0$ in two of the three reasonable equilibria. Model QQM is not that related to model LLM, but nevertheless, the analytical results obtained for model LLM are used as a base for numerical investigations for model QQM. Results are again illustratively shown for parameter set u_{opt} and initial mass $S = 15$ mmol N m^{-3}.

4.3.1. Model LQM

The first two equilibrium solutions of model LQM, solutions $E^*_{LQM_1}$ and $E^*_{LQM_2}$, are equal to the ones of model LLM. By implication, the corresponding linearizations and the associated eigenvalues coincide and thus, respective results presented for model LLM hold also for model LQM.

Fig. 4 shows the equilibria to which numerical solutions of model LQM converges to, at the top for varied parameter ϕ_P, at the bottom for varied parameter ϕ_Z. Notations and critcal values are as in Figs. 1 and 3, respectively. Caused by the lack of an analytic expression for solution $E^*_{LQM_3}$, symbolic computations of the associated eigenvalues are not possible. The other eigenvalues coincide with the ones for model LLM as mentioned (see Figs. 1 and 3).

Looking at the top plots in Figs. 1 and 4, it is clear that the stable domains of the respective equilibria with respect to the parameter ϕ_P are the same for both models. This means in particular that the critical points, where the quality of the solutions change, are the same. A first stability shift, from $E^*_{LQM_3}$ to $E^*_{LQM_2}$, occurs at $C_3(\phi_P)$. A second shift happens at $C_1(\phi_P)$ and $E^*_{LQM_1}$ is stable for all $\phi_P > C_1(\phi_P)$ (cp. Section 4.2).

The variation in ϕ_Z also shows similarities of the solutions stability for both models. Looking at the bottom plot in Fig. 4, a quality shift from solution E_{LQM_3} to solution E_{LQM_2} is observed at the critical point $C_2(\phi_Z)$, which is observed for model LLM as well (cp. Fig. 3). However, in contrast to model LLM, limit cycles do not appear in model LQM.

Similar to model LLM, variations in μ_m and k_N do not show remarkable new characteristics of the solutions. Furthermore, the stable ranges of the individual solutions coincide again for model LLM and model LQM. The co-existence solution is stable for all settings of k_N and the variation in μ_m shows that equilibrium $E^*_{LQM_1}$ is stable for very small values of μ_m, while equilibrium E_{LQM_3} is stable for values $\mu_m > C_1(\mu_m) \sim 0.042$.

The described observations can be explained as follows: On the one hand, the similarities are explained by the fact that the first two equilibria of the two models are equally defined. Thus, the third equilibrium is related to the quality of the other two equilibria which especially explains the simultaneous quality shifts of both models. On the other hand, the two models can differ in features that are independent of the first two solutions, because solution E^*_3 is specific for each model. This concerns for example the occurrence of limit cycles. While for model LLM there is a range of ϕ_Z where limit cycles occur, for model LQM limit cycles do not occur in the same situation. However, one can see that the classification presented for model LLM in Table 2 holds for model LQM as well.

4.3.2. Model QQM

The model QQM underlying formulation differs from the one of model LLM and LQM. Thus, it is not clear whether the classification presented in Table 2 is relevant for model QQM as well. However, since the first equilibrium of model QQM coincides the one of the other two models and further, the respective formulations differ just slightly (cp. Eqs. (2.1) and (2.2)), it is expected that model QQM shows some similar dynamical behaviour. To see to what extent model QQM resembles the dynamics of the other two models, comperative numerical experiments are conducted.

Fig. 5 shows the equilibrium solutions of model QQM, for varying ϕ_P at the top and varying ϕ_Z at the bottom. Comparing these two plots with the plots in Fig. 4, it is conspicuous that the solutions of model LQM and model QQM are similar for large parameter ranges of ϕ_P and ϕ_Z. Especially, the stability domains of the individual equilibria seem to agree for both models. Considering, e.g., the variation in ϕ_P, there are similar stability shifts from $E^*_{QQM_3}$ to $E^*_{QQM_2}$ and from $E^*_{QQM_2}$ to $E^*_{QQM_1}$ as observed for the other two models. The only difference is that the former shift does not occur at the critical point $C_3(\phi_P)$, introduced for model LLM, but at a point nearby. The critical value $C_3(\phi_P)$ is related to the eigenvalues arising from linearization $J_1(E^*_{LLM_2})$ which do not agree with the ones of $J_2(E^*_{QQM_2})$. A slight shift of the critical value from $C_3(\phi_P)$ to $C'_3(\phi_P) \sim 0.8128$ is the result.

The detected critical values with respect to k_N and μ_m are obtained from Eq. (3.10). Thus they are valid for model QQM as well and experiments for k_N and μ_m consequently show that the stability domains of the equilibria coincide with the ones for model LQM while varying these parameters. Further critical values, that could cause nevertheless a quality change, seem not to exist, at least

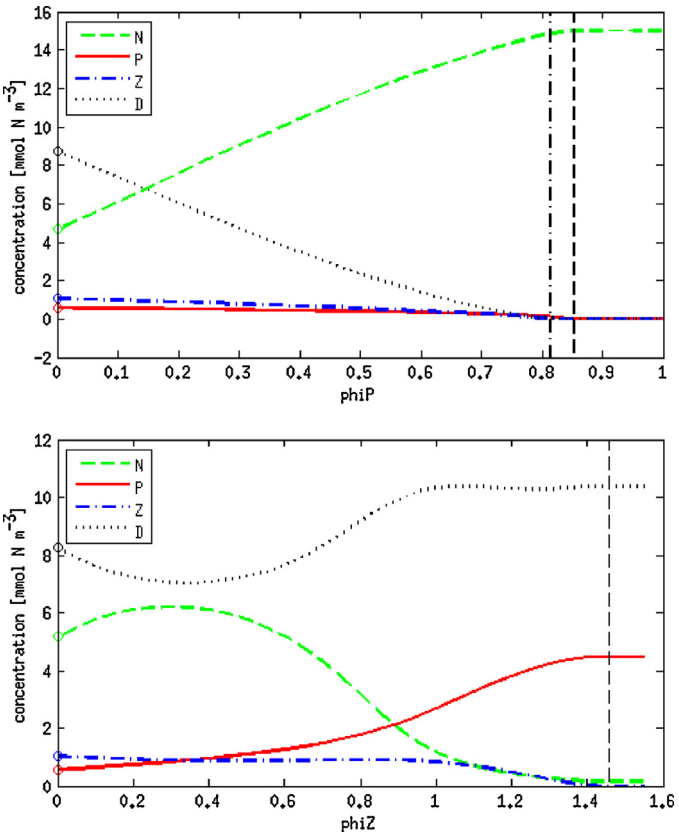

Fig. 5. As Fig. 4 for model QQM. The vertical lines mark the critical values $C(\phi_P)$ and $C(\phi_Z)$, respectively, that are detectable for model QQM.

not when using the parameter setting u_{opt}. Finally, the variation in the for model QQM specific parameter ϕ_P^* does not show a specific dynamical behaviour.or stability shifts. Independent of ϕ_P^*, solution $E^*_{QQM_3}$ is stable.

Thus, the biggest difference between model LQM and model QQM seems not to be in the stability ranges, but more in the respective solutions. As shown in Heinle and Slawig (2013) for variable initial masses, the individual solutions of model LQM and model QQM here also show interesting similarities and differences in the distribution of the individual tracer quantities. E.g., looking at the bottom plots of Figs. 4 and 5, both models converge to their co-existence equilibrium for a wide range of ϕ_Z. For around $\phi_Z \in (0, 1)$, the solutions are even similar in their respective quality and quantities. For $\phi_Z > 1$, the discrepancy between the solutions increases. The co-existence solution of each model converges continuously to the respective second equilibrium and, at least for parameter set u_{opt}, those two solutions differ significantly. While in model LQM the state of P exceeds the state of D, in model QQM it is the other way around. For varying μ_m and k_N the solutions of the two models differ only slightly.

5. Summary

Knowing the basic dynamics of a model it is possible to confidently decide whether a model is appropriate for a target purpose or not. In this paper a theoretically based method is presented to identify the possible dynamics of a model, which is exemplary shown for three typical, hierarchical structured formulations of NPZD type models.

For the simplest model formulation a classification of its dynamics depending on crucial parameter and initial value constellations could be introduced. This classification is theoretically based on analytical computations of the equilibria of the model as well as on a stability analysis of those using the linearization approach. As one eigenvalue of these linearizations is constantly 0, the absolute validity of the classification for the model itself is not given. To identify its reasonability for the actual nonlinear model, model LLM, as well as to examine its signifiance for the other two related model formulations, model LQM and QQM, numerical methods are applied.

The analytical computations for model LLM indicate the main significance of the parameters ϕ_P, μ_m, $k_N\beta$, g and ϕ_Z for its dynamics. Those determine whether an equilibrium is reasonable and stable, and thus significant for the model solution and its dynamics. In accordance to our analytical findings, numerical experiments are performed for variations of the mentioned parameters which show that the classification holds for the nonlinear model. Furthermore, the experiments revealed that limit cycles can appear for model LLM. This explains the feature of periodic oscillations that sometimes occur applying the model. Explicit conditions for their appearance, however, cannot be given since this feature is related to the quality of the co-existence equilibrium, which is analytically not examinable.

Numerical experiments with respect to the other two model formulations, model LQM and QQM, showed that (1) the classification presented for model LLM is true for model LQM as well; (2) model LQM and model QQM do not show limit cycles; (3) the difference of the model formulations do not result in significant differences of the stability ranges of the individual equilibrium solutions, but in quantitative differences between the model solutions; and (4) the dynamics of model LQM and model QQM differ only slightly.

6. Conclusions

Our study shows that the theoretical analyze of a simplified model is extremely worthwhile when the original model seems to be too complex for such an analytical approach. Statements obtained for the simplified model can be also used as theoretical base for numerical investigations of the more complex model. Furthermore, the results of our study show that differences in the model formulation, especially complications, do not necessarily imply completely different dynamics of the respective solutions. Thus, determining the dynamics of different model formulations helps to prudently detect a formulation matching the system to be simulated, and in particular, to find the simplest one of those.

The method presented in this study is easily transferable to other models, which is not restricted to marine ecosystem models. A confident application of a model is ensured in almost every domain knowing the dynamics of the model and their dependence on the formulation and parameters included.

Appendix A.

A.1.

The expressions for the equilibrium states of nutrients, zooplankton and detritus in solution $E^*_{LLM_3}$ are

$$N_3^*(S,u) = -[\theta_1 - ((\theta_1 + \gamma_m k_N \phi_Z - \gamma_m \phi_Z S)^2 + 4\gamma_m k_N \phi_Z(\gamma_m \phi_Z S - \gamma_m \phi_Z \theta_2 + \beta\gamma_m \phi_P \theta_2 - \beta \phi_P \phi_Z p_3^*))^{1/2} + \gamma_m k_N \phi_Z - \gamma_m \phi_Z S] \cdot [2\gamma_m \phi_Z]^{-1},$$

$$Z_3^*(S,u) = \frac{\beta\left(\phi_P + [\mu_m\theta_2\ \ ]\cdot\left[2\gamma_m\phi_Z\left(k_N - \frac{\theta_2}{2\gamma_m\phi_Z}\right)\right]^{-1}\right)P_3^*}{\phi_Z},$$

$$D_3^*(S,u) = \frac{\left(\beta\phi_P + [\mu_m(\beta-1)\theta_2]\cdot\left[2\gamma_m\phi_Z\left(k - \frac{\theta_2}{2\gamma_m\phi_Z}\right)\right]^{-1}\right)P_3^*}{\gamma_m}$$

where

$$\theta_1 = P_3^*(\gamma_m\phi_Z + \phi_Z\mu_m - \beta\gamma_m\phi_P + \beta\gamma_m\mu_m + \beta\phi_P\phi_Z - \beta\phi_Z\mu_m),$$

$$\theta_2 = \theta_3 + \gamma_m\phi_Z(k_N - S) - ((\theta_3 + \gamma_m k_N\phi_Z - \gamma_m\phi_Z S)^2 + 4\gamma_m k_N\phi_Z(\gamma_m\phi_Z S - \gamma_m\phi_Z P_3^* + \beta\gamma_m\phi_P P_3^* - \beta\phi_P\phi_Z P_3^*))^{1/2},$$

$$\theta_3 = P_3^*\cdot(\gamma_m\phi_Z + \phi_Z\mu_m - \beta\gamma_m\phi_P + \beta\gamma_m\mu_m + \beta\phi_P\phi_Z - \beta\phi_Z\mu_m).$$

A.2.

The Jacobian of ODE system (2.1) for model LQM is given by

$$J_{LQM} = \begin{pmatrix} -\frac{\mu_m k_N P}{(k_N+N)^2} & -\frac{\mu_m N}{k_N+N} & \phi_Z & \gamma_m \\ \frac{\mu_m k_N P}{(k_N+N)^2} & \frac{\mu_m N}{k_N+N} - \phi_P - \frac{2g^2\epsilon pZ}{(g+\epsilon p^2)^2} & -\frac{g\epsilon P^2}{g+\epsilon P^2} & 0 \\ 0 & \frac{\beta 2g^2\epsilon PZ}{(g+\epsilon P^2)^2} & \frac{\beta g\epsilon P^2}{g+\epsilon P^2} - \phi_Z - 2\phi_Z^* Z & 0 \\ 0 & \frac{(1-\beta)2g^2\epsilon PZ}{(g+\epsilon P^2)^2} + \phi_P & \frac{(1-\beta)g\epsilon P^2}{g+\epsilon P^2} + 2\phi_Z^* Z & -\gamma_m \end{pmatrix}.$$

A.3.

The Jacobian of ODE system (2.2) is given by

$$J_{QQM} = \begin{pmatrix} -\frac{\mu_m k_N P}{(k_N+N)^2} & \phi_P - \frac{\mu_m N}{k_N+N} & \phi_Z & \gamma_m \\ \frac{\mu_m k_N P}{(k_N+N)^2} & \frac{\mu_m N}{k_N+N} - \phi_P - 2\phi_p^* P - \frac{2g^2\epsilon PZ}{(g+\epsilon P^2)^2} & -\frac{g\epsilon P^2}{g+\epsilon P^2} & 0 \\ 0 & \frac{\beta 2g^2\epsilon Z}{(g+\epsilon P^2)^2} & \frac{\beta g\epsilon P^2}{g+\epsilon P^2} - \phi_Z - 2\phi_Z^* Z & 0 \\ 0 & \frac{(1-\beta)2g^2\epsilon PZ}{(g+\epsilon p^2)^2} + 2\phi_p^* P & \frac{(1-\beta)g\epsilon P^2}{g+\epsilon P^2} + 2\phi_Z^* Z & -\gamma_m \end{pmatrix}.$$

References

Amann, H., 1990. Ordinary Differential Equations: An Introduction to Nonlinear Analysis. Walter de Gruyter, Berlin, Germany.

Fasham, M.J.R., Flynn, K.J., Pondaven, P., Anderson, T.R., Boyd, P.W., 2006. Development of a robust marine ecosystem model to predict the role of iron in biogeochemical cycles: a comparison of results for iron-replete and iron-limited areas, and the SOIREE iron-enrichment experiment. Deep Sea Research I 53, 333–366.

Fennel, K., Losch, M., Schröter, J., Wenzel, M., 2001. Testing a marine ecosystem model: sensitivity analysis and parameter optimization. Journal of Marine Research 28, 45–63.

Fennel, W., Neumann, T.e., 2004. Introduction to the Modelling of Marine Ecosystems (Elsevier Oceanography Series 72). Elsevier, Amsterdam, The Netherlands.

Gregg, W.W., Ginoux, P., Schopf, P.S., Casey, N.W., 2003. Phytoplankton and iron: validation of a global three-dimensional ocean biogeochemical model. Deep Sea Research II 50, 3143–3169.

Heinle, A., Slawig, T., 2013. Internal dynamics of NPZD type ecosystem models. Ecological Modelling 254, 33–42.

Kidston, M., Matear, R., Baird, M.E., 2011. Parameter optimisation of a marine ecosystem model at two contrasting stations in the Sub-Antarctic ZoneT. Deep Sea Research II 58, 2301–2315.

Moore, J.K., Doney, S.C., Glover, D.M., Fung, I.Y., 2002. Iron cycling and nutrient-limitation patterns in surface waters of the World Ocean. Deep Sea Research II 49, 463–507.

Oschlies, A., Garçon, V., 1999. An Eddy-permitting coupled physical–biological model of the North Atlantic. 1. Sensitivity to advection numerics and mixed layer physics. Global Biogeochemical Cycles 13, 135–160.

Rückelt, J., Sauerland, V., Slawig, T., Srivastav, A.B.W., Patvardhan, C., 2010. Parameter optimization and uncertainty analysis in a model of oceanic CO_2 uptake using a hybrid algorithm and algorithmic differentiation. Nonnlinear Analysis: Real World Applications 11, 3993–4009.

Schartau, M., Oschlies, A., 2003. Simultaneous data-based optimization of a 1D-ecosystem model at three locations in the north Atlantic: part I – method and parameter estimates. Journal of Marine Research 61, 765–793.